

Probing heavy scalar in supersymmetric final states




Amit Adhikary
Indian Institute of Science, Bengaluru, India

Based on

JHEP 04 (2021) 284, with Biplob Bhattacharjee, Rohini M. Godbole, Najimuddin Khan
and Suchita Kulkarni

SUSY 2021, 23-28 August, 2021, Online

Introduction

- The last missing piece in SM, Higgs boson, has been discovered at the LHC in 2012 whose properties are more or less consistent with Standard Model.
 - There are many reasons for exploring beyond the SM (BSM) physics: gauge hierarchy, dark matter, neutrino mass, baryon asymmetry etc.
 - A very well motivated model to search for BSM particles is the Minimal Supersymmetric extension of the SM (MSSM).
 - lepton (e) or quark (u) \rightarrow slepton (\tilde{e}) or squark (\tilde{u})
 - gauge boson (g, W^\pm, W^0, B^0) \rightarrow gaugino ($\tilde{g}, \tilde{W}^\pm, \tilde{W}^0, \tilde{B}^0$)
 - five Higgs bosons (h, H, A, H^\pm)
 - Higgs ($H_u^+, H_u^0, H_d^0, H_d^-$) \rightarrow Higgsino ($\tilde{H}_u^+, \tilde{H}_u^0, \tilde{H}_d^0, \tilde{H}_d^-$)
 - $\tilde{B}^0, \tilde{W}^0, \tilde{H}_u^0, \tilde{H}_d^0 \rightarrow \tilde{\chi}_1^0, \tilde{\chi}_2^0, \tilde{\chi}_3^0, \tilde{\chi}_4^0$ (neutralino)
 - $\tilde{W}^\pm, \tilde{H}_u^\pm, \tilde{H}_d^\pm \rightarrow \tilde{\chi}_1^\pm, \tilde{\chi}_2^\pm$ (chargino)
- 
- The diagram shows two horizontal lines on the left, one above the other. A vertical line descends from the top line and a vertical line ascends from the bottom line, meeting at a central point. From this central point, a horizontal arrow points to the right, ending at the text 'Electroweakinos'.

Motivation and objective of the work

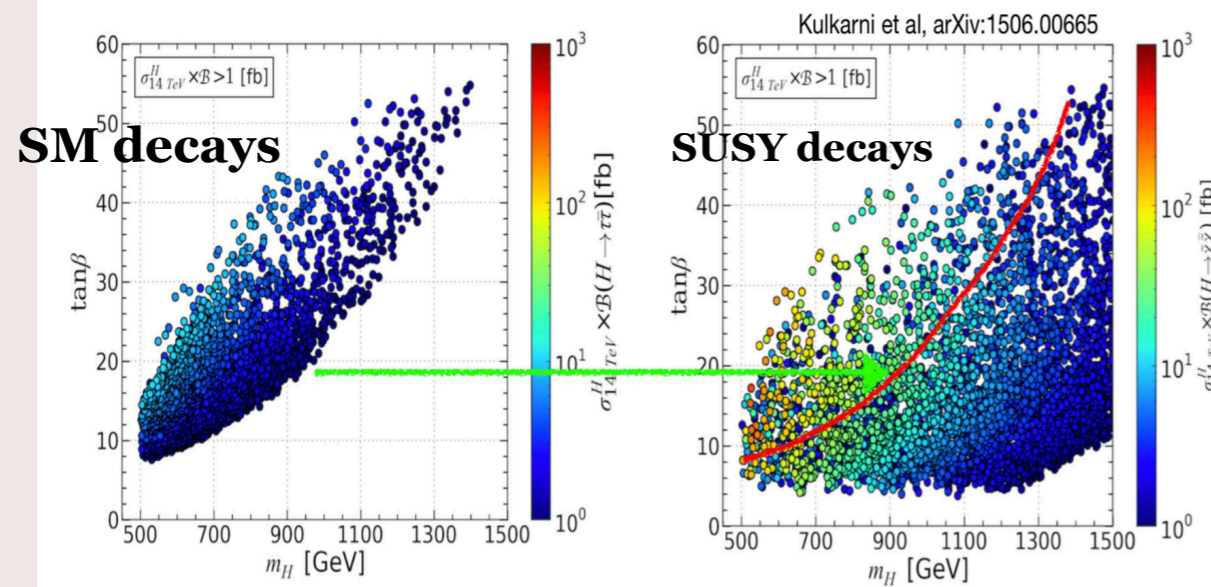
slide borrowed from talk by Prof. Godbole, [link-talk](#)

Light LSP and Heavy Higgs!

Heavy Higgs into electroweakinos

Heavy Higgs into electroweakinos complementary to SM final states.

(See also: Arbey et al. arXiv:1303.7450, Barman et al. arXiv:1607.00676, Bagnaschi arXiv:1808.07542).



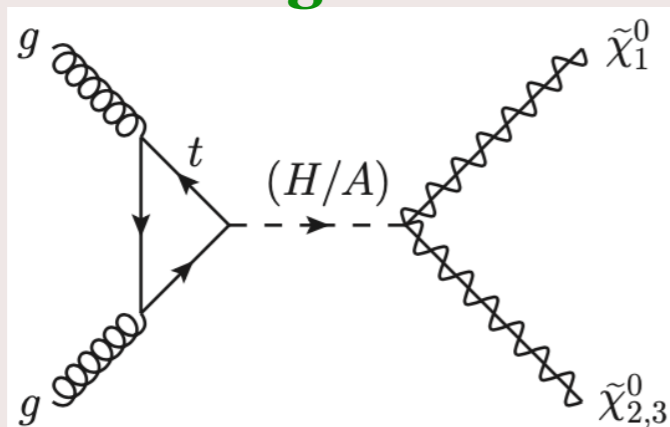
SUSY 2021, Beijing, 23-28 Aug

August 23, 2021

- When kinematically allowed, heavy Higgs can also decay to electroweakinos.
- There is a nice complementarity between high $\tan\beta$ regime, where the $pp \rightarrow b\bar{b}H, H \rightarrow \tau\tau$ becomes dominant, and, high m_H and low $\tan\beta$ regime, where $H \rightarrow \text{susy/ electroweakinos}$ become important.

Signal!

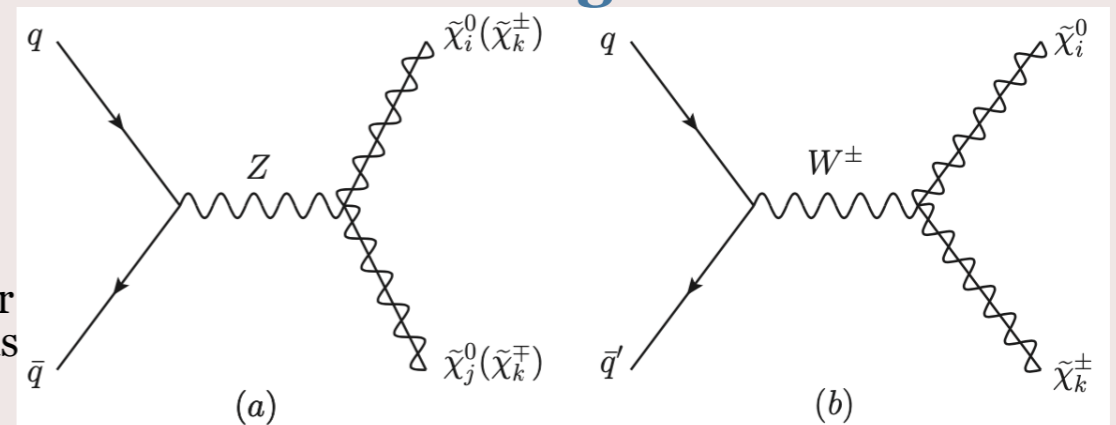
Resonant electroweakino production:



Direct electroweakino production:

Along with other SM Backgrounds

New Background!



Benchmark Study

Heavy Higgs coupling to electroweakinos is maximised when the gaugino and higgsino component is sizeable in the electroweakinos.

Playing with gaugino and higgsino content of the electroweakinos!

CASE-1:

Other fixed parameters:

$$M_A = 1 \text{ TeV}, 4 < \tan\beta < 20, M_3 = 5 \text{ TeV}, A_t = -5 \text{ TeV},$$

$$A_{e,\mu,\tau,u,d,c,s,b} = 0, M_{\tilde{e}_L,\tilde{\mu}_L,\tilde{\tau}_L,\tilde{e}_R,\tilde{\mu}_R,\tilde{\tau}_R} = 5 \text{ TeV},$$

$$M_{\tilde{Q}_{1L},\tilde{Q}_{2L},\tilde{Q}_{3L}} = 5 \text{ TeV}, M_{\tilde{u}_R,\tilde{d}_R,\tilde{c}_R,\tilde{s}_R,\tilde{t}_R,\tilde{b}_R} = 5 \text{ TeV}.$$

- Case1: $M_2 = 1.5 \text{ TeV}, \mu = 450 \text{ GeV}$
- Case1a: $M_1 = 370 \text{ GeV}$
- Dominant decays: $H \rightarrow \tilde{\chi}_1^0 \tilde{\chi}_2^0, \tilde{\chi}_1^0 \tilde{\chi}_3^0, \tilde{\chi}_1^0 \tilde{\chi}_1^0;$
 $\tilde{\chi}_{2,3}^0 \rightarrow Z \tilde{\chi}_1^0$ (mono-Z + E_T)
- Case1b: $M_1 = 300 \text{ GeV}$
- $\tilde{\chi}_2^0 \rightarrow Z \tilde{\chi}_1^0$ (mono-Z + E_T), $\tilde{\chi}_3^0 \rightarrow h \tilde{\chi}_1^0$ (mono-h + E_T)
- Case1c: $M_1 = 100 \text{ GeV}$
- $\tilde{\chi}_2^0 \rightarrow h \tilde{\chi}_1^0$ (mono-h + E_T), $\tilde{\chi}_3^0 \rightarrow Z \tilde{\chi}_1^0$ (mono-Z + E_T)

No constraints applied except SM Higgs mass between [122,128] GeV

Mass hierarchy:

———— Wino
 ————— Higgsino
 ————— Bino

Our Interest

Benchmark Study

CASE-2:

- Case2: $M_1 = 300$ GeV, $M_2 = 400$ GeV, $\mu = 350$ GeV
- Mixed scenario \rightarrow heavy Higgs to any $\tilde{\chi}_i^0/\tilde{\chi}_j^\pm$ pair

Mass hierarchy:

Degenerate
 ——— Wino
 ——— Higgsino
 ——— Bino

$$\tilde{\chi}_2^0 (\tilde{\chi}_3^0) \rightarrow \tilde{\chi}_1^0 + \ell^+ + \ell^- \quad (BR \sim 6.15 (9.84) \%)$$

$$\tilde{\chi}_2^0 (\tilde{\chi}_3^0) \rightarrow \tilde{\chi}_1^0 + q + \bar{q} \quad (BR \sim 40.47 (64.52) \%)$$

$$\tilde{\chi}_2^0 (\tilde{\chi}_3^0) \rightarrow \tilde{\chi}_1^0 + \nu + \bar{\nu} \quad (BR \sim 12.36 (19.71) \%)$$

$$\tilde{\chi}_2^0 (\tilde{\chi}_3^0) \rightarrow \tilde{\chi}_1^0 + \gamma \quad (BR \sim 3.09 (1.86 \times 10^{-2}) \%)$$

$$\tilde{\chi}_1^\pm \rightarrow \tilde{\chi}_1^0 + q + \bar{q}' \quad (BR \sim 66.80 \%)$$

$$\tilde{\chi}_1^\pm \rightarrow \tilde{\chi}_1^0 + \ell + \nu \quad (BR \sim 33.28 \%)$$

(2/3/4)-lepton + \cancel{E}_T , 2-lepton + jets + \cancel{E}_T , 2-lepton + γ + \cancel{E}_T , 2γ + \cancel{E}_T etc.

multi-lepton + \cancel{E}_T , multi-jet + \cancel{E}_T , lepton + jets + \cancel{E}_T etc.

Benchmark Study

CASE-3:

- Case3: $M_1 = 1 \text{ TeV}$, $M_2 = 300 \text{ GeV}$, $\mu = 500 \text{ GeV}$
- Long lived wino-like $\tilde{\chi}_1^\pm$ (LLCP=Long lived charged particle)

Mass hierarchy:

———— Bino

———— Higgsino

———— Wino

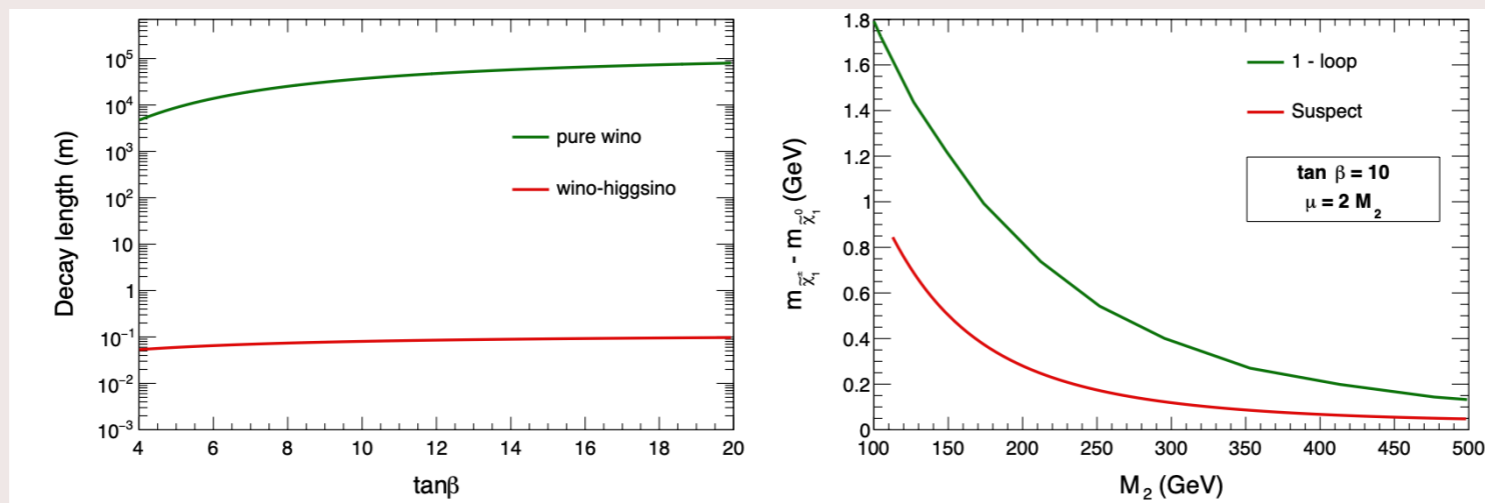


Figure 5: Decay length of a charged wino in pure wino state (green) and mixed state of wino-higgsino (red) in Suspect2 (left), and comparison of mass splitting ($\Delta m_{\tilde{\chi}_1^\pm - \tilde{\chi}_1^0}$) between Suspect2 and 1-loop result [38] (right).

1-loop result: Nuclear Physics B, 559(1):27 – 47, 1999

Scanning MSSM parameter space

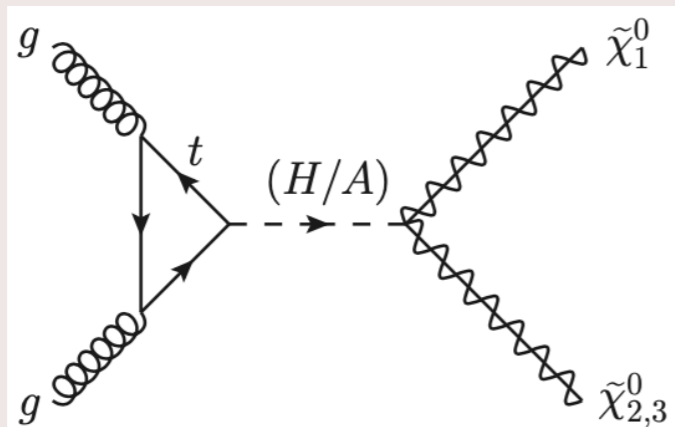


Fig. **Resonant** electroweakino production. Electroweakinos must have gaugino and higgsino component to couple to Higgs boson.

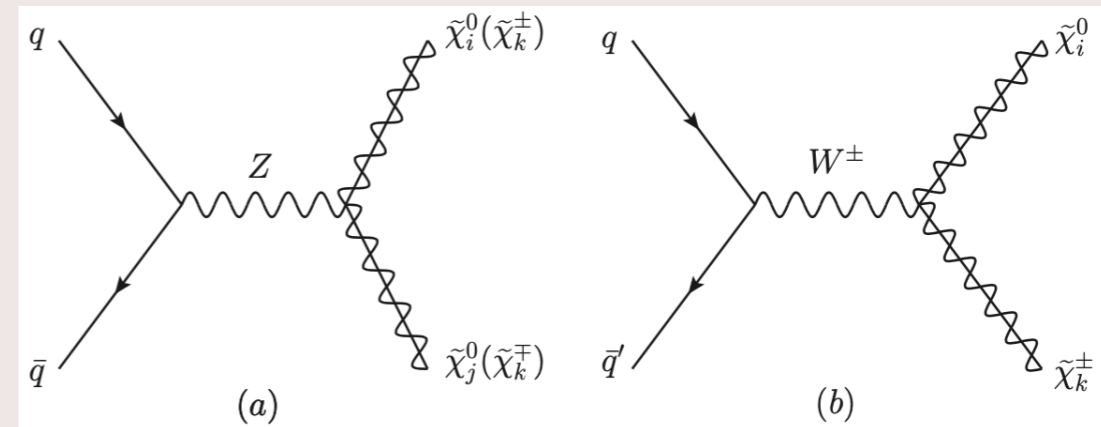


Fig. **Direct** electroweakino production.

- Allowed MSSM parameter space \rightarrow Random scan + Experimental Constraints
- Experimental Constraint: Higgs signal strength, heavy Higgs searches, LEP constraints, dark matter direct detection, flavour physics.
- Tools: Suspect, SusyHit (Hdecay, Sdecay), MicroOMEGA (HiggsSignal, HiggsBound, Direct Detection), SModelS, SusyAI

Kinematics of mono-(Z/h) final states

- Mono-Z + \cancel{E}_T :

- $pp \rightarrow H \rightarrow \tilde{\chi}_1^0 \tilde{\chi}_2^0, \tilde{\chi}_2^0 \rightarrow Z \tilde{\chi}_1^0, Z \rightarrow \ell^+ \ell^-$
- $pp \rightarrow \tilde{\chi}_1^0 \tilde{\chi}_2^0, \tilde{\chi}_2^0 \rightarrow Z \tilde{\chi}_1^0, Z \rightarrow \ell^+ \ell^-$

- $L_T = p_{T,\ell 1} + p_{T,\ell 2} + \cancel{E}_T$

- $\xi = |p_{T,\ell\ell} - \cancel{E}_T| / p_{T,\ell\ell}$

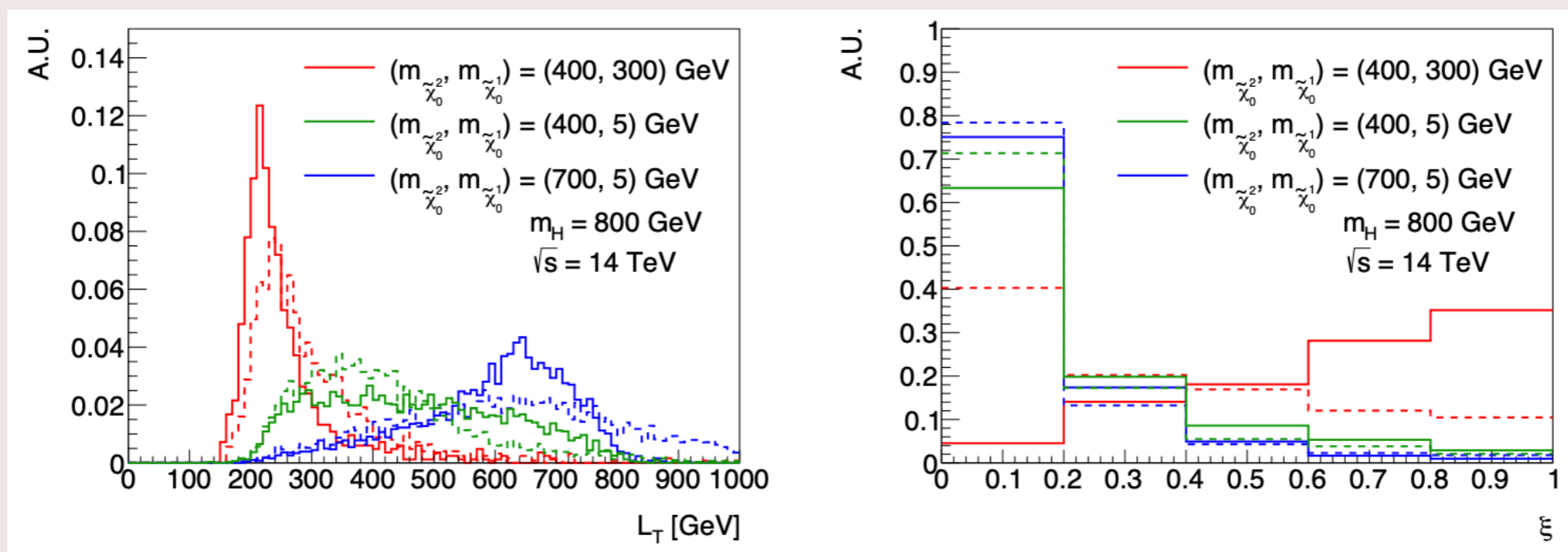


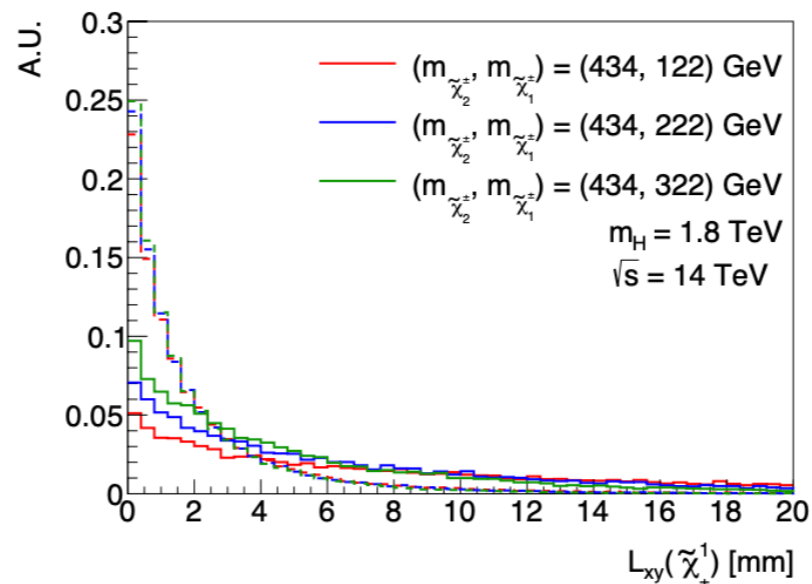
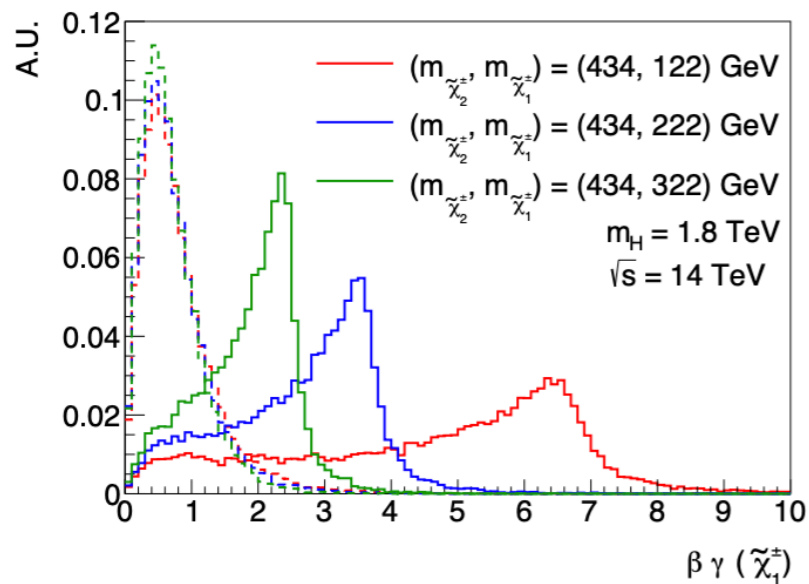
Fig. Normalised distributions of L_T and ξ .

Case-1 in slide-4

Kinematics of mono-(Z/h) final states

- Boosted charginos:**

- $pp \rightarrow H \rightarrow \tilde{\chi}_1^\pm \tilde{\chi}_2^\pm, \tilde{\chi}_2^\pm \rightarrow W^\pm \tilde{\chi}_1^0, \tilde{\chi}_1^\pm \rightarrow \tilde{\chi}_1^0 W^*$
- $pp \rightarrow \tilde{\chi}_1^\pm \tilde{\chi}_1^\pm, \tilde{\chi}_1^\pm \rightarrow \tilde{\chi}_1^0 W^*$



Charginos can travel more distance because of the boost received from heavy Higgs.

Fig. Normalised distributions of chargino boost and resulting displacement.

Case-3 in slide-6

Collider search

- Signal: **Mono-X (X=Z/h)** signatures arising from, $pp \rightarrow H/A \rightarrow \tilde{\chi}_1^0 + (\tilde{\chi}_{2,3}^0), (\tilde{\chi}_{2,3}^0) \rightarrow \tilde{\chi}_1^0 + (Z/h),$
 - $Z \rightarrow ll : ll + \cancel{E}_T$
 - $h \rightarrow b\bar{b} : b\bar{b} + \cancel{E}_T$
 - $h \rightarrow \gamma\gamma : \gamma\gamma + \cancel{E}_T$
- Two benchmark points are chosen for analysis :
 1. $M_A = 650 \text{ GeV}, \tan\beta = 10.80$
 2. $M_A = 750 \text{ GeV}, \tan\beta = 12.10$
 - with the common parameters,

$$M_1 = 5.04 \text{ GeV}, M_2 = 1.06 \text{ TeV}, \mu = 243.24 \text{ GeV}, M_3 = 2 \text{ TeV}, A_t = -3.65 \text{ TeV}, A_\tau = -1.44 \text{ TeV},$$

$$M_{\tilde{Q}_{1L}, \tilde{Q}_{2L}} = M_{\tilde{u}_R, \tilde{d}_R, \tilde{c}_R, \tilde{s}_R} = M_{\tilde{e}_L, \tilde{\mu}_L, \tilde{\nu}_R, \tilde{\mu}_R} = 3 \text{ TeV}, M_{\tilde{Q}_{3L}} = 4.91 \text{ TeV}, A_b = -1.11 \text{ TeV}, A_{e,\mu,u,d,c,s} = 0,$$

$$M_{\tilde{\tau}_L} = 961.52 \text{ GeV}, M_{\tilde{\tau}_R} = 1.07 \text{ TeV}, M_{\tilde{t}_R} = 5.91 \text{ TeV}, M_{\tilde{b}_R} = 2 \text{ TeV}.$$

$ll + \cancel{E}_T$ Channel

Signal :

$$pp \rightarrow H/A \rightarrow \tilde{\chi}_1^0 + (\tilde{\chi}_{2,3}^0), \quad (\tilde{\chi}_{2,3}^0) \rightarrow \tilde{\chi}_1^0 + Z, \quad Z \rightarrow \ell\ell$$

Two production modes: $gg \rightarrow H, pp \rightarrow b\bar{b}H$

Backgrounds :

- **SUSY** : $pp \rightarrow \tilde{\chi}_1^0\tilde{\chi}_{2,3}^0, \tilde{\chi}_1^\pm\tilde{\chi}_{2,3}^0, \tilde{\chi}_2^0\tilde{\chi}_3^0$
- **SM** : ZZ, WZ, VVV, $t\bar{t}Z$ and $t\bar{t}$

b-veto

b-tag

Optimised fixed

Selection cuts	
BP 1	BP 2
$2\ell, N_b = 0$ $76.0 < m_{\ell\ell} < 106.0$ $ \eta_{\ell\ell} < 2.5$ $N_j \leq 1$	
$\Delta R_{\ell\ell} < 1.3$ $\Delta\phi_{\ell\ell, \cancel{E}_T} > 2.1$ $\cancel{E}_T > 180 \text{ GeV}$ $\xi < 0.4$	$\Delta R_{\ell\ell} < 1.5$ $\Delta\phi_{\ell\ell, \cancel{E}_T} > 2.1$ $\cancel{E}_T > 210 \text{ GeV}$ $\xi < 0.3$

Selection cuts	
BP 1	BP 2
$2\ell, N_b \geq 1$ $76.0 < m_{\ell\ell} < 106.0$ $ \eta_{\ell\ell} < 2.5$ $N_j \leq 1$	
$\Delta R_{\ell\ell} < 1.3$ $\Delta\phi_{\ell\ell, \cancel{E}_T} > 2.1$ $\cancel{E}_T > 160 \text{ GeV}$ $\xi < 0.4$	$\Delta R_{\ell\ell} < 1.3$ $\Delta\phi_{\ell\ell, \cancel{E}_T} > 2.3$ $\cancel{E}_T > 170 \text{ GeV}$ $\xi < 0.8$

$ll + \cancel{E}_T$ Channel

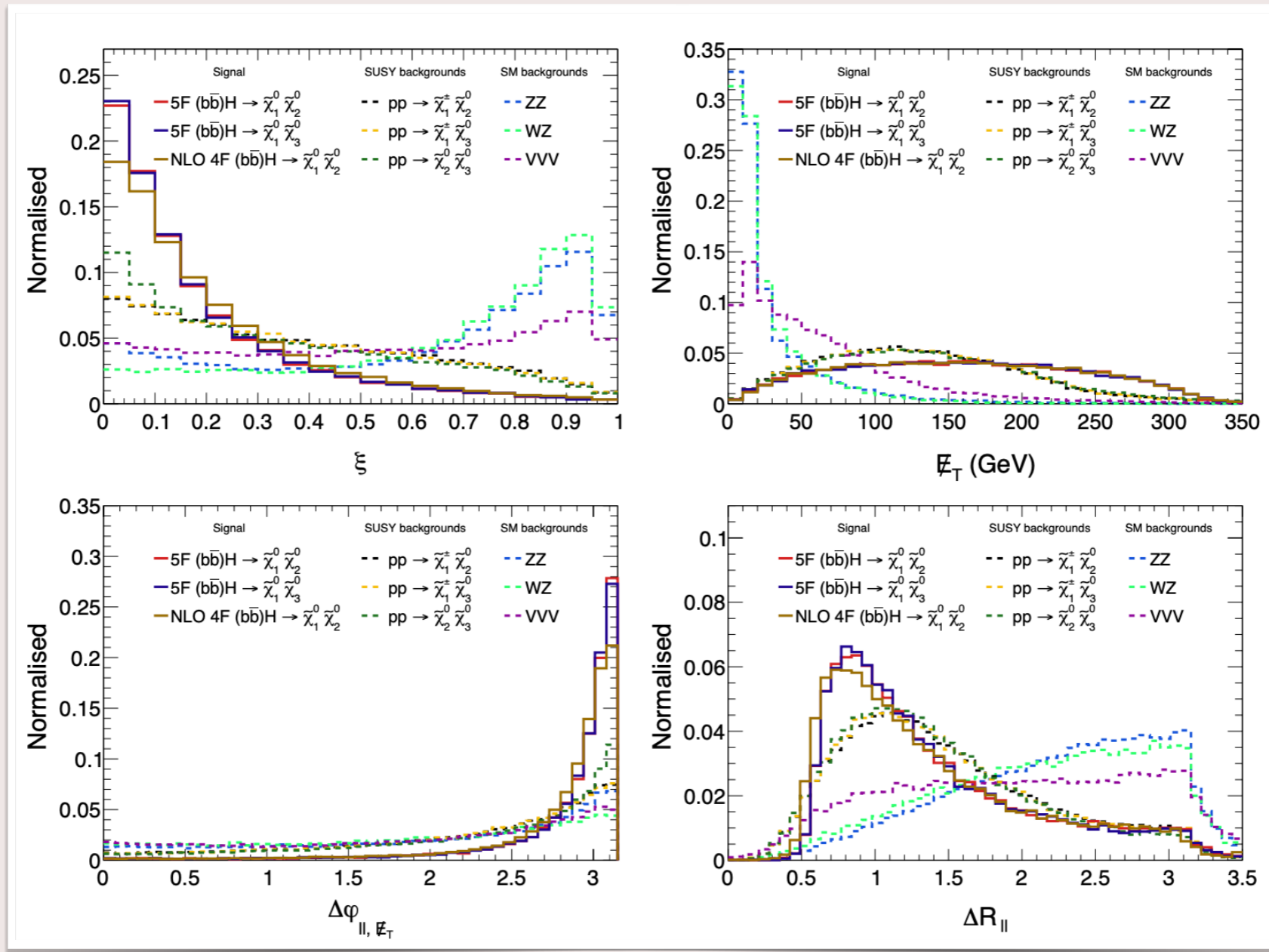


Fig. Normalised distributions of the optimised kinematic variables.

Result from all search Channels

1. $ll + \cancel{E}_T$ channel:

- S/\sqrt{B} = b-veto analysis: 6.57 (BP1), 4.66 (BP2); b-tag analysis: 10.48 (BP1), 8.03(BP2)
- b-tag category improves the result up to $\sim 70\%$.

2. $b\bar{b} + \cancel{E}_T$ channel:

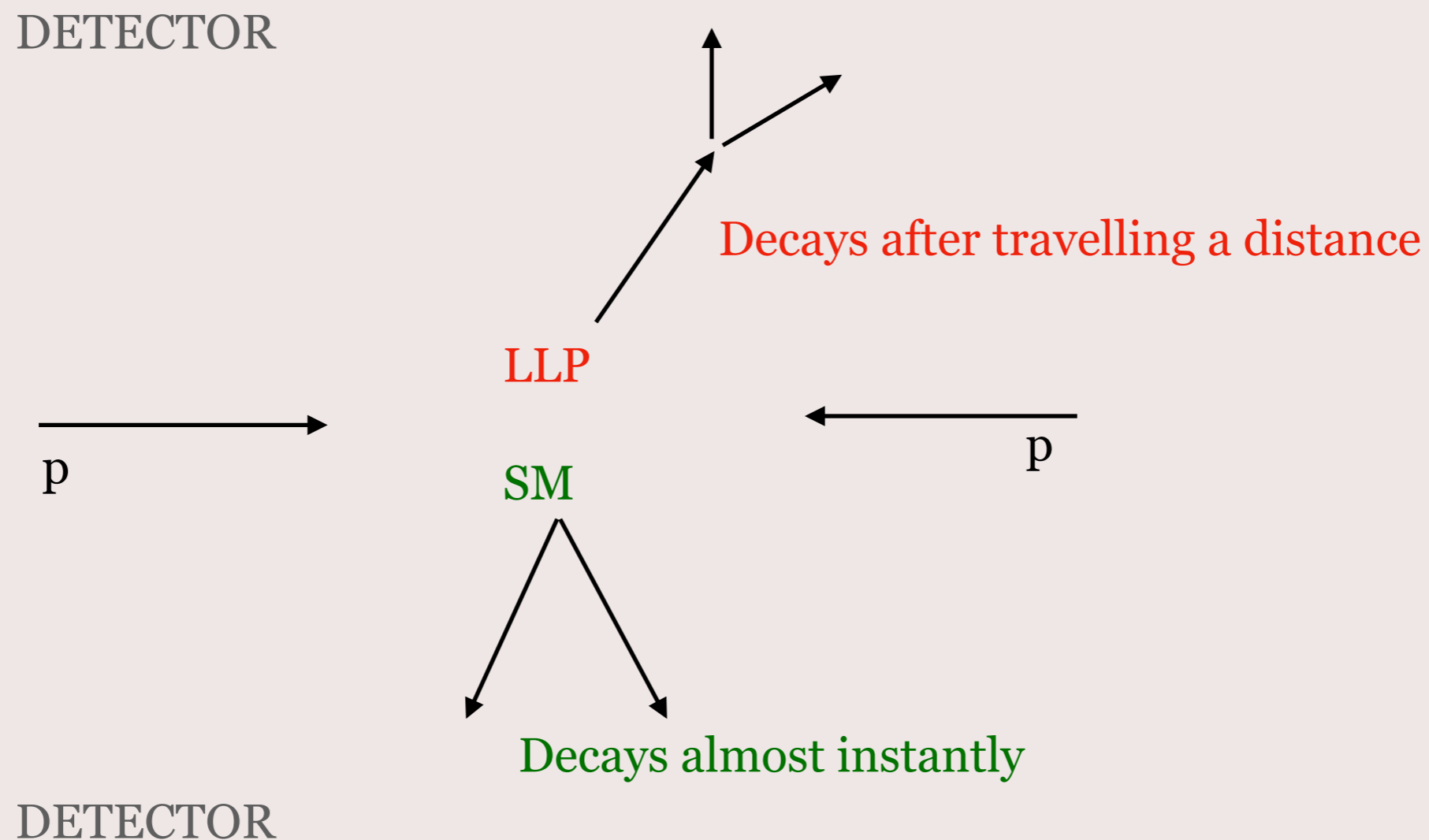
- S/B is poor, large $t\bar{t}$, $Zb\bar{b}$ background.
- S/\sqrt{B} = b-veto analysis: 7.25 (BP1), 5.94 (BP2); b-tag analysis: 3.93 (BP1), 3.70(BP2)

3. $\gamma\gamma + \cancel{E}_T$ channel:

- small event yield, but clean final state.

Susy backgrounds can have significant contribution and overlap with the signal kinematic distribution.

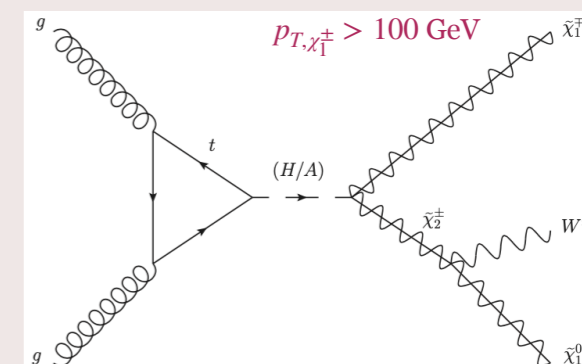
Long-lived particle (LLP)



Probing neutral Higgs in LLCP decay

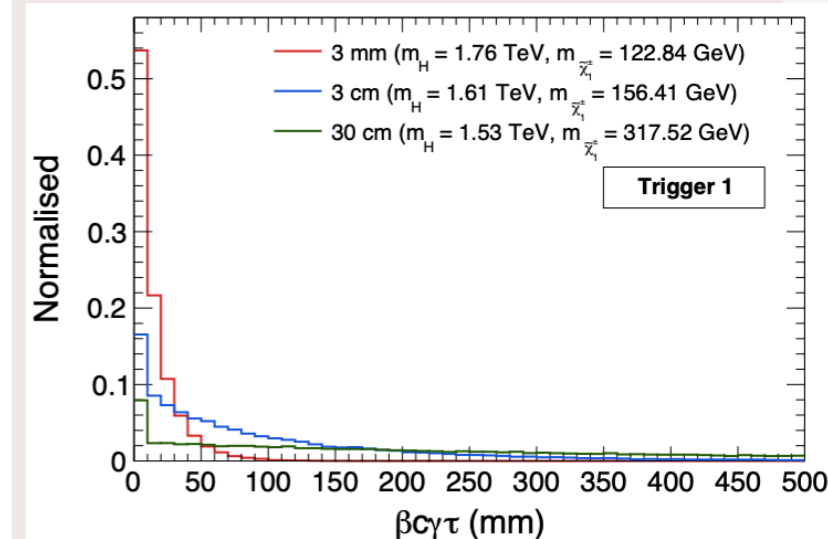
- $pp \rightarrow H \rightarrow \tilde{\chi}_1^\pm \tilde{\chi}_2^\pm$, $\tilde{\chi}_2^\pm \rightarrow W^\pm \tilde{\chi}_1^0$ **[Long-lived charged particle]**
- **Good track reconstruction [12,30] cm [JHEP 06 (2018) 022, ATL-PHYS-PUB-2019-011]**
- 3 benchmark points with chargino decay length 3 mm, 3 cm and 30 cm.

Trigger	Cuts
Trigger 1	$p_{T,e} > 30 \text{ GeV}$, $ \eta_e < 2.5$
Trigger 2	At least one jet with $p_T > 200 \text{ GeV}$ and $ \eta < 2.5$
Trigger 3	At least two jets with $p_T > 150 \text{ GeV}$ and $ \eta < 2.5$



Boosted $\tilde{\chi}_1^\pm \rightarrow$ more distance

Trigger cuts	$\beta c\gamma\tau$ of $\tilde{\chi}_1^\pm$	Fraction of events after trigger in % within					
		0 – 3 mm	3 – 30 mm	30 mm - 10 cm	10 – 30 cm	30 – 100 cm	> 100 cm
Trigger 1	3 mm	26.61	59.49	13.58	0.32	0.0	0.0
	3 cm	9.83	22.56	32.53	28.48	6.57	0.03
	30 cm	6.16	6.27	14.07	27.99	35.27	10.24
Trigger 2	3 mm	24.07	60.49	15.10	0.34	0.0	0.0
	3 cm	9.49	19.44	31.62	31.89	7.51	0.05
	30 cm	5.86	6.01	13.64	27.66	36.39	10.44
Trigger 3	3 mm	23.06	60.75	15.86	0.33	0.0	0.0
	3 cm	9.03	18.01	31.58	32.79	8.53	0.06
	30 cm	5.90	5.63	13.04	27.07	37.53	10.83



Probing charged Higgs in LLCP decay

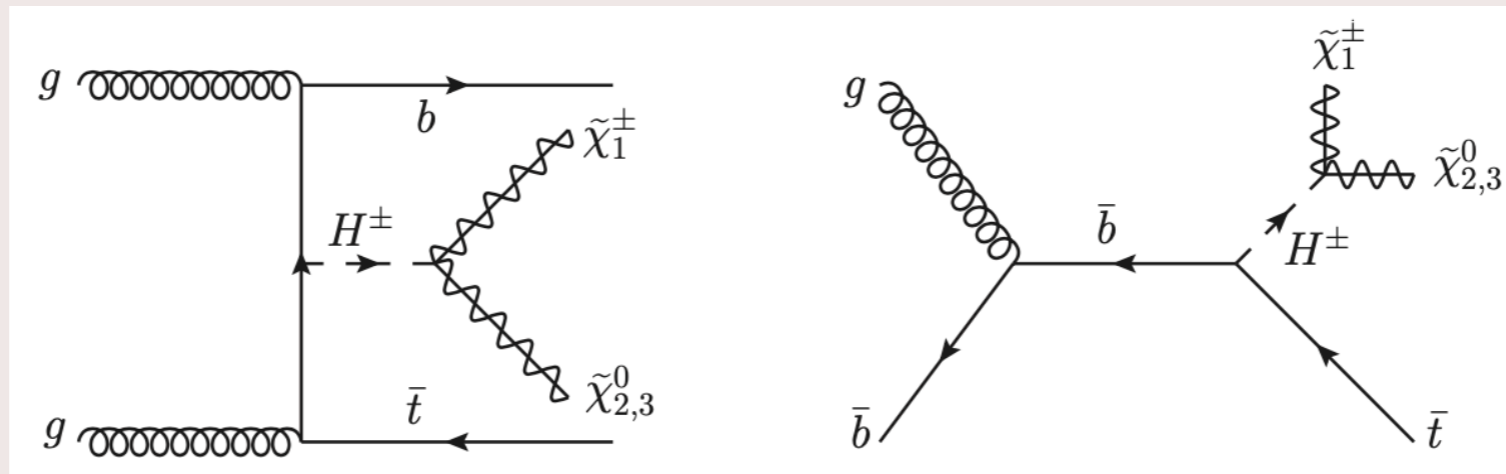


Fig. Feynman diagrams of charged Higgs production.

- $pp \rightarrow H^\pm (b\bar{t}/\bar{t})$, $H^\pm \rightarrow \tilde{\chi}_1^\pm \tilde{\chi}_{2,3}^0$, $\tilde{\chi}_{2,3}^0 \rightarrow \tilde{\chi}_1^0 (Z/h)$
- 3 benchmark points chosen with, $m_{H^\pm} \sim 620, 820$ and 1077 GeV
- 3 channels : (1) $Z \rightarrow ll$, (2) $h \rightarrow b\bar{b}$, (3) $h \rightarrow \gamma\gamma$

ll+LLCP Channel

$$H^\pm \rightarrow \tilde{\chi}_1^\pm \tilde{\chi}_{2,3}^0, \quad \tilde{\chi}_{2,3}^0 \rightarrow \tilde{\chi}_1^0 + (Z \rightarrow \ell\ell),$$

$$H^\pm \rightarrow \tilde{\chi}_2^\pm \tilde{\chi}_1^0, \quad \tilde{\chi}_2^\pm \rightarrow \tilde{\chi}_1^\pm + (Z \rightarrow \ell\ell).$$

Trigger Z	m_{H^\pm} (GeV)	Total event yield from the processes in equation 5.7 at 3 ab^{-1}	
		before Trigger Z	after Trigger Z
$p_{T,\ell_{1,2}} > 25 \text{ GeV}, \eta_{\ell_{1,2}} < 2.5,$ $76 \text{ GeV} < m_{\ell\ell} < 106 \text{ GeV},$ $p_{T,b} > 30 \text{ GeV}, \eta_b < 2.5$	620.29	427.04	173.12
	819.77	262.40	119.54
	1077.18	101.91	47.98

Table 29: The event yield at 3 ab^{-1} from all the processes before and after, applying trigger cuts and $p_{T,\tilde{\chi}_1^\pm} > 100 \text{ GeV}, |\eta_{\tilde{\chi}_1^\pm}| < 2.5$.

m_{H^\pm} (GeV)	$\beta c\gamma\tau$ of $\tilde{\chi}_1^\pm$ (cm)	Fraction of events after Trigger Z in % within					
		0 – 3 mm	3 – 30 mm	30 mm - 10 cm	10 – 30 cm	30 – 100 cm	> 100 cm
620.29	27.66	0.91	6.90	16.22	31.31	36.09	8.57
819.77	18.10	0.90	7.94	16.97	32.75	33.86	7.58
1077.18	3.7	4.07	28.75	37.55	24.98	4.60	0.05

Table 30: The fractional number of events which decay at different parts inside tracker for the $4F$ production process with $H^\pm \rightarrow \tilde{\chi}_2^\pm \tilde{\chi}_1^0$ in $\ell\ell + \text{LLCP}$ category.

$b\bar{b} + \text{LLCP}$ Channel

$$H^\pm \rightarrow \tilde{\chi}_1^\pm \tilde{\chi}_{2,3}^0, \tilde{\chi}_{2,3}^0 \rightarrow \tilde{\chi}_1^0 + (h \rightarrow b\bar{b}),$$

$$H^\pm \rightarrow \tilde{\chi}_2^\pm \tilde{\chi}_1^0, \tilde{\chi}_2^\pm \rightarrow \tilde{\chi}_1^\pm + (h \rightarrow b\bar{b}).$$

Trigger hbb	m_{H^\pm} (GeV)	Total event yield from the processes in equation 5.8 at 3 ab^{-1}	
		before Trigger hbb	after Trigger hbb
$p_{T,b_{1,2}} > 30 \text{ GeV}, \eta_{b_{1,2}} < 2.5,$ $90 \text{ GeV} < m_{bb} < 130 \text{ GeV},$ $0.4 < \Delta R_{bb} < 2.0$	620.29	3060.04	238.06
	819.77	1801.37	169.75
	1077.18	649.55	68.58

Table 31: Summarising the trigger cuts (additional cut: $p_{T,\tilde{\chi}_1^\pm} > 100 \text{ GeV}$ and $|\eta_{\tilde{\chi}_1^\pm}| < 2.5$) and the event yield at 3 ab^{-1} in the $b\bar{b} + \text{LLCP}$ category.

m_{H^\pm} (GeV)	$\beta c\gamma\tau$ of $\tilde{\chi}_1^\pm$ (cm)	Fraction of events after Trigger hbb in % within					
		0 – 3 mm	3 – 30 mm	30 mm - 10 cm	10 – 30 cm	30 – 100 cm	> 100 cm
620.29	27.66	6.43	7.86	16.55	31.49	32.08	5.59
819.77	18.10	6.09	8.96	17.59	31.27	30.00	6.09
1077.18	3.7	10.55	31.13	34.07	20.67	3.54	0.04

Table 32: The fractional number of events which decay at different parts inside tracker for the $4F$ production process with $H^\pm \rightarrow \tilde{\chi}_2^\pm \tilde{\chi}_1^0$ in $b\bar{b} + \text{LLCP}$ category.

$\gamma\gamma$ +LLCP Channel

$$H^\pm \rightarrow \tilde{\chi}_1^\pm \tilde{\chi}_{2,3}^0, \tilde{\chi}_{2,3}^0 \rightarrow \tilde{\chi}_1^0 + (h \rightarrow \gamma\gamma),$$

$$H^\pm \rightarrow \tilde{\chi}_2^\pm \tilde{\chi}_1^0, \tilde{\chi}_2^\pm \rightarrow \tilde{\chi}_1^\pm + (h \rightarrow \gamma\gamma).$$

Trigger $h\gamma\gamma$	m_{H^\pm} (GeV)	Total event yield from the processes in equation 5.9 at 3 ab^{-1}	
		before Trigger $h\gamma\gamma$	after Trigger $h\gamma\gamma$
$p_{T,\gamma_{1,2,b}} > 30 \text{ GeV}, \eta_{\gamma_{1,2,b}} < 2.5,$ $122 \text{ GeV} < m_{\gamma\gamma} < 128 \text{ GeV},$ $0.4 < \Delta R_{\gamma\gamma} < 2.0$	620.29	11.93	3.65
	819.77	7.03	2.38
	1077.18	2.53	0.87

Table 33: Summarising the trigger cuts (additional cuts applied on $\tilde{\chi}_1^\pm$: $p_{T,\tilde{\chi}_1^\pm} > 100 \text{ GeV}$ and $|\eta_{\tilde{\chi}_1^\pm}| < 2.5$) and the event yield at 3 ab^{-1} in the $\gamma\gamma + \text{LLCP}$ category.

m_{H^\pm} (GeV)	$\beta c\gamma\tau$ of $\tilde{\chi}_1^\pm$ (cm)	Fraction of events after Trigger $h\gamma\gamma$ in % within					
		0 – 3 mm	3 – 30 mm	30 mm - 10 cm	10 – 30 cm	30 – 100 cm	> 100 cm
620.29	27.66	0.89	7.71	16.30	31.60	35.56	7.94
819.77	18.10	0.90	8.22	17.46	31.95	34.28	7.19
1077.18	3.7	3.93	29.98	37.70	24.41	3.94	0.04

Table 34: The fractional number of events which decay at different parts inside tracker for the $4F$ production process with $H^\pm \rightarrow \tilde{\chi}_2^\pm \tilde{\chi}_1^0$ in $\gamma\gamma + \text{LLCP}$ category.

Conclusion

- Hierarchy in the gaugino and higgsino content inside electroweakinos can give rise to many interesting final states for collider searches.
- We studied distinct kinematic features for resonant and direct susy production.
- We performed a collider search for heavy Higgs in electroweakino final states. The susy backgrounds are important along with the SM backgrounds. Tagging additional b-jet will improve the final signal significance.
- A wino-like chargino is long-lived. If it comes from the decay of a heavy Higgs boson, it can be can travel more distance because of the boost received from heavy Higgs. We quantified the fraction of long-lived charginos with respect to their decay length in lab frame. Further, this can improve the sensitivity of disappearing track searches at the LHC.

Thank you for your attention!